



## Application Note SC-XRD 514

# D8 VENTURE METALJET

- GPCR Crystallography Moves In-House: Structure of the Human Orexin-1 StaR<sup>®</sup> to 2.77 Å

### Introduction

Here we present the first reported structure of a GPCR solved from diffraction data collected on a home-lab X-ray system. The structure of the human Orexin-1 StaR<sup>®</sup> (Stabilized Receptor) was solved at 2.77 Å resolution in a monoclinic space group using data collected on the D8 VENTURE METALJET in just over 2½ hours.

The unique combination of the Bruker METALJET and PHOTON II technologies, in concert with the Heptares StaR<sup>®</sup> technology, synergize to enable collection of diffraction data from GPCR crystals at a resolution high enough for Structure-Based Drug Design (SBDD).

## GPCRs: Key targets for structure-based drug discovery

The G-Protein Coupled Receptor (GPCR) superfamily of membrane proteins represents one of the most difficult for structure determination due to their conformational heterogeneity and inherent instability when removed from their native cell membrane environment. GPCRs, expressed in every cell in the human body, use a canonical transmembrane 7-helix bundle to act as a delicate molecular rheostat for transmission of signals across the cell membrane. Of the more than 120,000 structures submitted to the RCSB PDB, less than 0.15% are GPCR structures, and yet this superfamily of proteins is the site of action of 25-30% of all current drugs on the market.

To date, all GPCR structures deposited in the PDB have been determined exclusively by X-ray crystallography using state-of-the-art synchrotron beamlines or XFEL sources [REF1].

## GPCRs and StaR technology

As a result of groundbreaking work from a handful of groups globally, the last decade has witnessed a near-exponential increase in available GPCR structural information. Of all the GPCR structures present in the PDB, fully a third are driven by StaRs: the backbone of Heptares' integrated SBDD platform for targeting GPCRs.

A StaR is a GPCR with a small number of point mutations that greatly improve its thermostability without disrupting its pharmacology [REF2 – REF3]. StaR technology is transferrable across the GPCR superfamily, providing stable, functionally-relevant, purified conformations of target GPCRs that retain their expected drug-binding characteristics.

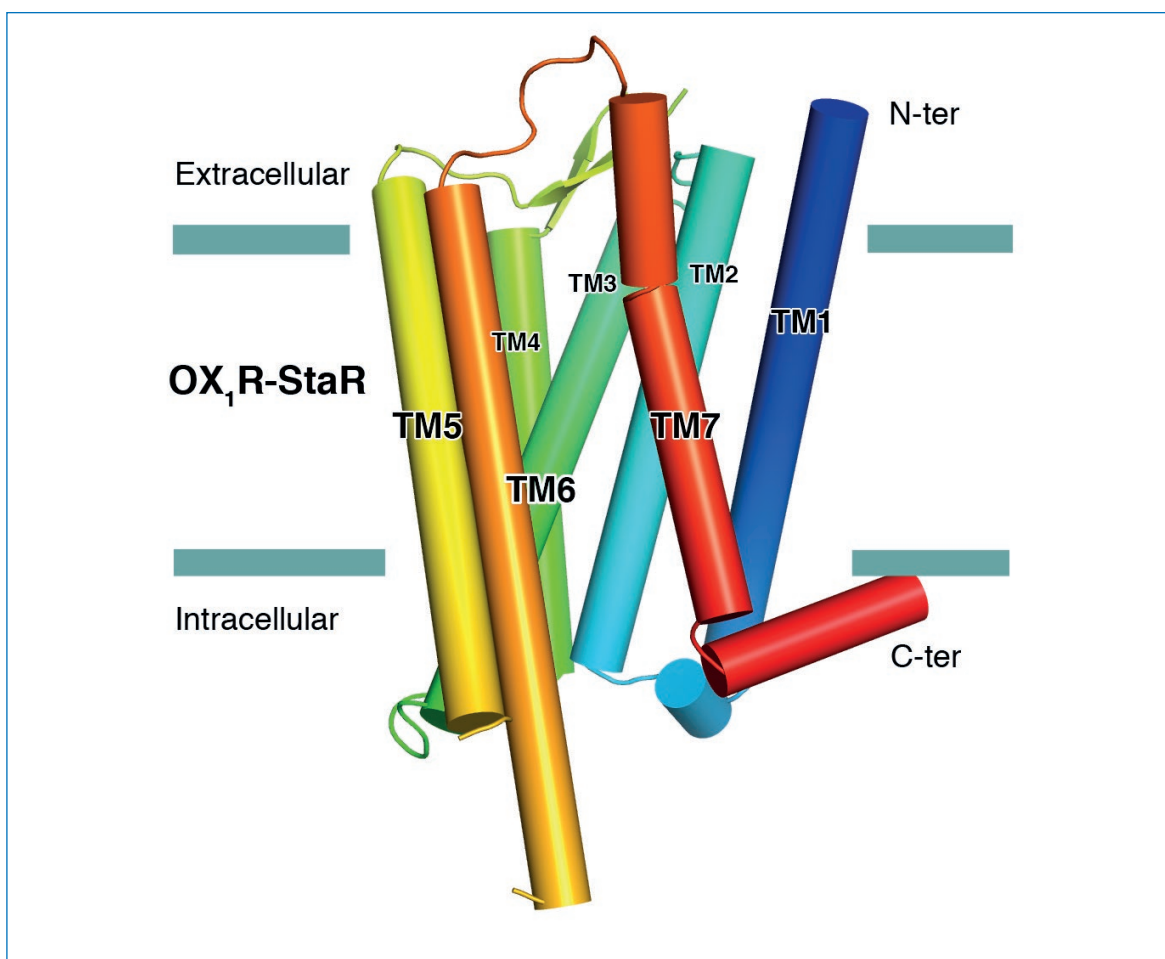


Figure 1: GPCR structure solved in-house to 2.77 Å resolution using D8 VENTURE METALJET. OX<sub>1</sub>-StaR in cylindrical helix representation. Approximate membrane boundaries are marked.

### In-house GPCR crystallography on D8 VENTURE with METALJET

SBDD organizations continue to use and rely on in-house systems to determine crystallographic structures due to their convenience in both usage and around-the-clock accessibility. On-site structure determination can provide fast turnaround times to medicinal chemists, enabling key decisions to be made quickly and efficiently in real time.

Joint feasibility studies between Bruker and Heptares have found that the D8 VENTURE with METALJET, together with StaR technology, can collect data at speeds and resolutions [ ] sufficient for a role in SBDD pipelines specifically dedicated to GPCRs.

The human orexin-1 (OX1/OX1-R) receptor antagonist project is a focus of the Heptares pipeline. It has indications for cocaine addiction and relapse, along with potential broad applications in substance addictions (e.g., nicotine and alcohol) and compulsive disorders (e.g., gambling and binge eating).

The D8 VENTURE's unique combination of features provided high-quality data on a single OX1-StaR crystal, enabling its solution at a final resolution of 2.77 Å.

Technology	Feature	Benefit for GPCR Crystallography
<b>METALJET X-ray source</b>	70-micron beam diameter	Maximizes diffraction from small crystals and minimizes background scatter
	Very high intensity	Increases diffraction intensity from weakly scattering crystal
	Extremely stable beam	Essential to minimize errors from small crystals
<b>KAPPA goniometer</b>	KAPPA goniometer (SoC < 7 microns)	Improves data accuracy from small crystals
	Multi-axis goniometer	Enables efficient data collection to minimize radiation damage and shorten measurement time
	Continuous crystal rotation enables shutterless data collection	Eliminate timing errors
<b>PHOTON II CPAD detector</b>	Single-photon sensitivity	Accurate measurement of weakest reflections
	Large active area and low point spread enables processing of samples with the largest unit cells	Enables data collection at longer crystal-detector distance to minimize noise from non-crystallographic scattering
	Dynamic oversampling provides a wide dynamic range	Accurate measurement of strong and weak reflections on single frame
<b>PROTEUM3 software suite</b>	Strategy determination	Calculates most efficient data collection strategy to avoid radiation damage
	SAINT+/SADABS	Enable accurate processing of finely-sliced data
	XPREP	Easy space group determination and preparation of output files

Table 1: Technical requirements for in-house single-crystal GPCR data collection.

## Experimental methods and results

### Crystal growth and screening

Crystals of the OX1-StaR, in complex with a new chemical entity (NCE), were grown using vapor diffusion methods and stored in liquid nitrogen. A total of 20 crystals were screened using the D8 VENTURE (Table 1) for their diffraction properties using 2 orthogonal five-degree wedges of data collected at an exposure rate of 30 s and 0.5°. The diffraction limit of the crystals was found to vary between 3.5 and 2.8 Å.

### Key features for GCPR in-house data collection

Data was collected at 100 K on a single crystal (Figure 2) of OX1-StaR using the D8 VENTURE with METALJET X-ray source, KAPPA goniometer, and PHOTON II CPAD detector.

The METALJET uses a gallium-rich liquid alloy target to produce X-rays. HELIOS MX graded-multilayer optics deliver a monochromatic beam of Ga-K $\alpha$  wavelength (1.34 Å, 9.2 KeV). Ga-K $\alpha$  has a slightly shorter wavelength than Cu K $\alpha$ , which reduces the amount of background scatter from air and water (~12% less compared to Cu), and produces a better S/N (signal-to-noise)—beneficial for weakly-diffracting crystals. The X-ray beam is tightly focused to a diameter of 70  $\mu$ m at the crystal position, which also enhances S/N from small crystals.

	OX1-StaR
Wavelength (Å)	1.3418
Crystal dimensions ( $\mu$ m)	80 $\times$ 80 $\times$ 50
Temperature (K)	100
Space group	P2 <sub>1</sub>
<i>a</i> , <i>b</i> , <i>c</i> (Å)	59.57, 146.43, 71.72
$\alpha$ , $\beta$ , $\gamma$ (°)	90.00, 112.38, 90.00
Mosaicity (°)	0.41
Detector distance (mm)	100
2 $\theta$ (°)	0
Scan type	Omega
Rotation range per image (°)	0.1
Exposure time per image (s)	6
Total rotation range (°)	162.6
Total measurement time	2 h 40 min

Table 2: Data collection parameters.

The PHOTON II CPAD detector's large active area boasts single-photon sensitivity and a highly uniform response. This proved essential for the accurate measurement of reflections produced by the OX1-StaR crystal. The PHOTON II operates in shutterless mode, enabling fine slices of data to be collected continuously.

Crystal indexing and determination of the optimal data collection strategy were performed by PROTEUM3 [REF4]. Finely-sliced data was collected at  $\sim$ 1/4 of the crystal mosaicity in order to accurately measure the reflection intensity profile in the rotation dimension and maximize S/N. Data was collected to 2.60 Å at a single detector position of 2 $\theta$  = 0° and a distance of 100 mm.

A total of 982.6° of data was collected. Radiation damage became apparent (as an increase in R<sub>meas</sub> [REF5]) after the first scan, and the data was cut at this point. The first 162.2° of data were processed, resulting in a 99.3% complete dataset with a redundancy of 3.21 (Table 2).

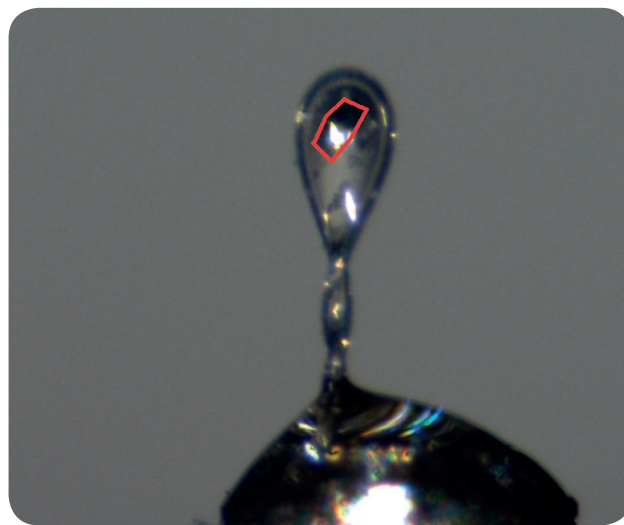


Figure 2: D8 VENTURE video image of the 80  $\times$  80  $\times$  50 micron GCPR crystal.

	OX1-StaR
Resolution limit (Å)	2.77 (2.87 – 2.77)
Total number of reflections	92,909
Number of unique reflections	28,725
Completeness (%)	99.3 (97.9)
Redundancy	3.21 (2.62)
$\langle I/\sigma(I) \rangle$	8.05 (1.05)
R <sub>r.i.m.</sub>	0.139 (0.775)

Table 3: Data processing statistics.

## Data processing

The OX1-StaR data was finally cut at 2.77 Å resolution, where  $CC_{1/2}$  was 50% and  $\langle I/\sigma I \rangle$  was 1.08. [REF6]. Data were integrated using SAINT+ [REF7], and merged and scaled using SADABS [REF8]. XPREP was used for space group determination and calculation of data statistics (Table 3).

## Structure determination

The structure of OX1-StaR was solved by molecular replacement using the program PHASER [REF9] from the CCP4 suite of programs [REF10]. An unpublished OX1-StaR structure (Heptares Therapeutics) served as the single search model. A solution was found and was validated through subsequent refinement. Initial refinement was carried out with REFMAC5 [REF 11] using maximum-likelihood restrained refinement in combination with the jelly-body protocol. Further and final stages of refinement were performed with PHENIX.REFINE [REF 12] with positional, individual isotropic B-factor refinement and TLS. Manual model building was performed in COOT [REF13].

The structure of the Orexin-1 receptor was solved to 2.77 Å. The structure (Figures 1, 3, 4) refined with good statistics  $R_{\text{cryst}}/R_{\text{free}} = 24.4\%/27.2\%$ . Refinement statistics are presented in Table 4.

OX1-StaR	
Resolution (Å)	2.77 (2.87 – 2.77)
Completeness (%)	99.3 (97.9)
$\sigma$ cutoff	1.4
Number of reflections, working set	27150
Number of reflections, test set	1575
Final $R_{\text{cryst}}$	0.2444
Final $R_{\text{free}}$	0.2721
Bonds (Å)	0.0038
Angles (°)	0.9798
Ramachandran plot	98.0

Table 4: Structure solution and refinement

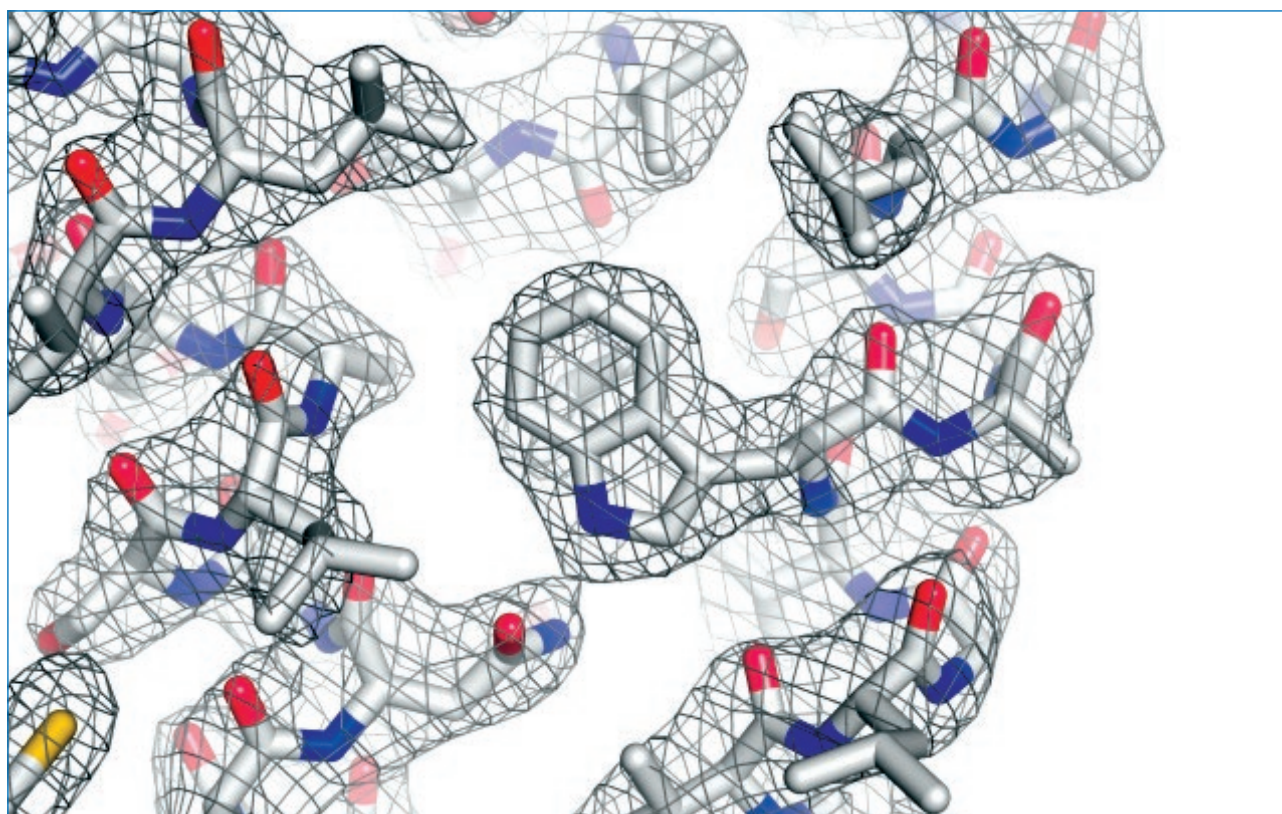


Figure 3: Representative  $2m|FO|-|DFC|$  density contoured at  $1.4\sigma$  showing the structure of a transmembrane helix of OX1-StaR at 2.77 Å resolution.

### Comparison of D8 VENTURE METALJET Structure with Synchrotron Structures

The refinement statistics of OX1-StaR collected on the D8 VENTURE have been compared with 158 GPCR structures deposited in the PDB (Figure 4). The PDB structures were all solved from synchrotron (154) or XFEL (4) data, and all are between 1.7 and 4.2 Å resolution. The OX1-StaR structure described here was solved at 2.77 Å—better than approximately 60% of synchrotron GPCR structures, and notably with comparable refinement statistics.

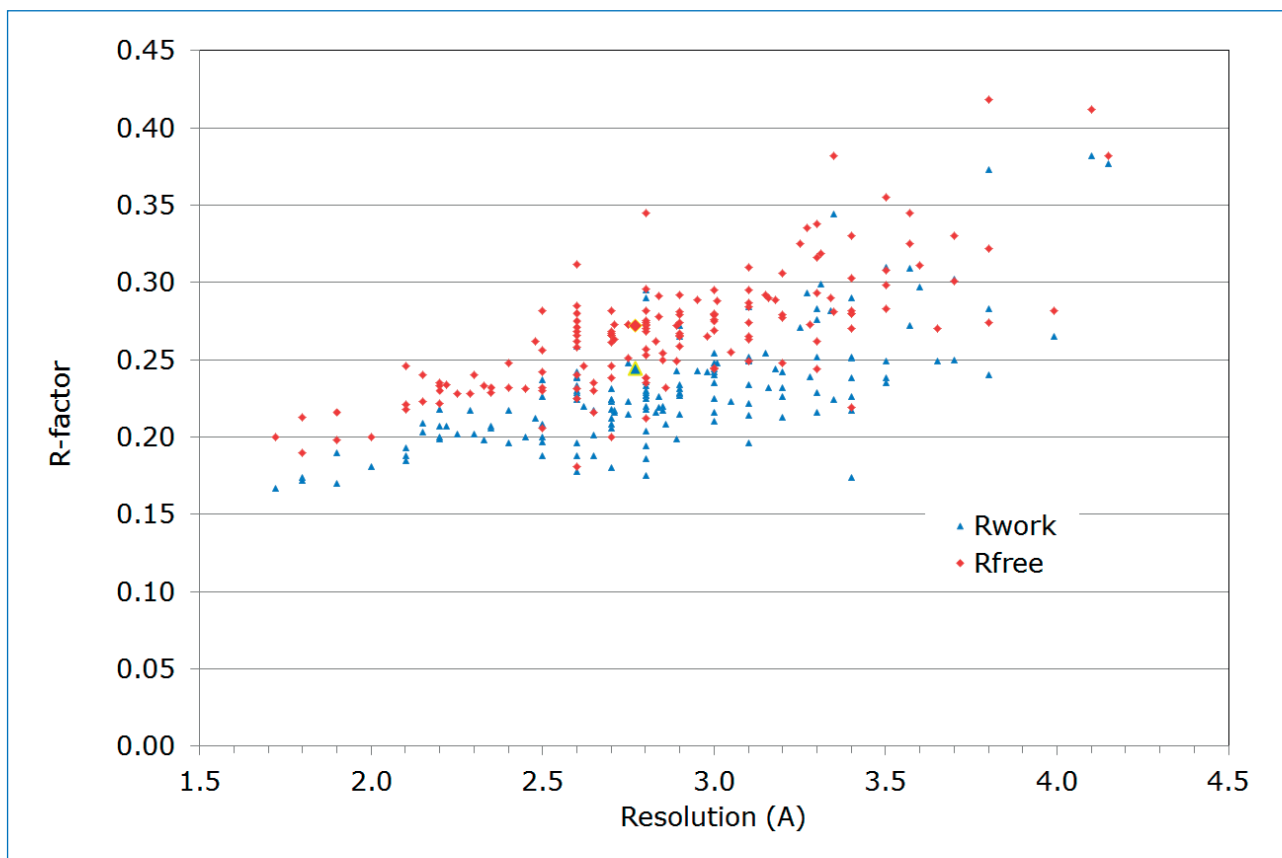


Figure 4: Comparison of in-house OX1-StaR structure with PDB entries solved at synchrotron and XFEL sources. The R factors for the D8 VENTURE METALJET structure are shown yellow framed.

## Conclusions

This report details the first GPCR structure solved using an in-house source, the D8 VENTURE. The structure was solved at 2.77 Å resolution, and a complete dataset for this low-symmetry primitive monoclinic system was collected in just over 2½ hours from a single crystal. This study (i.e., the feasibility of in-house GPCR structure determination for SBDD) owes its success to Heptares Therapeutics and Bruker's unique combination of technologies: the stabilized OX1-StaR and the D8 VENTURE with METALJET.

Heptares' StaR technology enables the generation of homogeneous populations of thermostabilized GPCRs in a conformation matching the drug product profile. Such thermostabilization opens avenues for GPCR crystallization (i.e., vapor diffusion in harsh, short-chain that would otherwise be closed using wild-type receptors). The growth of StaR crystals provides samples with sufficient diffraction quality for in-house single-crystal data collection.

The METALJET X-ray source delivers a high-intensity X-ray beam, yet a complete dataset can be collected from a single primitive monoclinic StaR GPCR crystal prior to the onset of radiation damage. Additionally, the use of a KAPPA goniometer with the large, single-photon-sensitive PHOTON II detector enables finely-sliced data to be collected efficiently without the need for multiple detector 2θ positions. Furthermore, the ability to collect a complete dataset from a single StaR crystal limits the introduction of error in the structure factors that can arise when merging data from multiple crystals that may not be perfectly isomorphous.

Together, the combined technologies of the StaR system and the D8 VENTURE make in-house GPCR crystallography a productive and attractive addition to the SBDD pipeline.

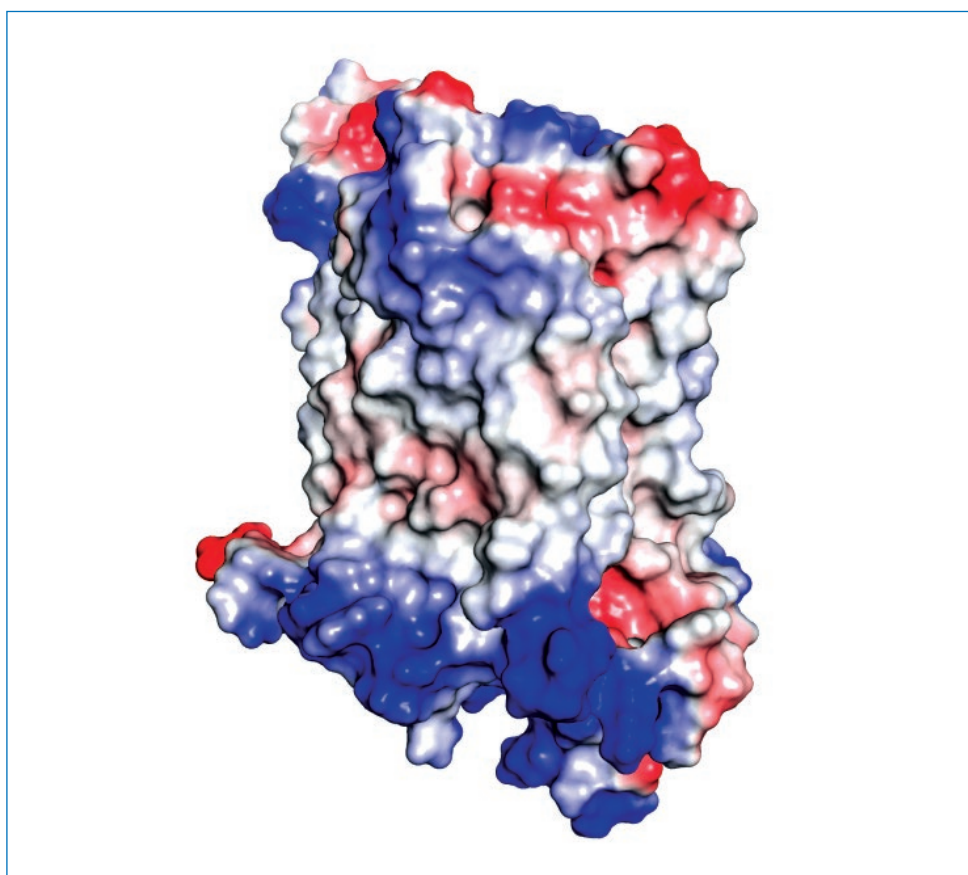


Figure 5: A surface charge representation of OX1-StaR demonstrates the hydrophobic belt (white) spanning the membrane bilayer with two bands of negatively-charged residues (red) aligned with the basic lipid head groups.

## References

1. Cooke, R. M. et al. Structures of G protein-coupled receptors reveal new opportunities for drug discovery. *Drug Discov. Today*. **20(11)**, 1355-64 (2015).
2. Serrano-Vega, M. J., Magnani, F., Shibata, Y. & Tate, C. G. Conformational thermostabilization of the beta1-adrenergic receptor in a detergent-resistant form. *Proc. Natl. Acad. Sci. USA*. **105**, 877-882 (2008).
3. Robertson, N. et al. The properties of thermostabilised G protein-coupled receptors (StaRs) and their use in drug discovery. *Neuropharmacology* **60**, 36-44 (2011).
4. Bruker AXS (2016). PROTEUM3, Version 2016.1, Bruker AXS Inc., Madison, Wisconsin, USA.
5. Diederichs, K. (2003) Some aspects of quantitative analysis and correction of radiation damage. *Acta Cryst.* **D62**, 96-101.
6. Karplus PA, Diederichs K: Linking crystallographic model and data quality. *Science* 2012, 336:1030-1033.
7. Schneider, T.R. and Sheldrick, G.M., (2002). *Acta Cryst.* **D58**, 1772-1779.
8. Sheldrick, G.M., (2002). *Z. Kristallogr.* **217**, 644–650.
9. McCoy, A. J. et al. Phaser crystallographic software. *J. Appl. Cryst.* **40**, 658-674 (2007). REFMAC
10. Collaborative Computational Project, Number 4 The CCP4 Suite: Programs for Protein Crystallography. *Acta Crystallogr. D Biol. Crystallogr.* **50**, 760-763 (1994).
11. Murshudov, G. N. et al. REFMAC5 for the refinement of macromolecular crystal structures. *Acta Crystallogr. D Biol. Crystallogr.* **67**, 355-367 (2011).
12. Afonine, P. V. et al. Towards automated crystallographic structure refinement with phenix.refine. *Acta Crystallogr. D Biol. Crystallogr.* **68**, 352-367 (2012).
13. Emsley, P., Lohkamp, B., Scott, W. G. & Cowtan, K. Features and development of Coot. *Acta Crystallogr. D Biol. Crystallogr.* **66**, 486-501 (2010).

## Authors

Severine Freisz, Vernon Smith, Bruker AXS GmbH, Karlsruhe, Germany

Andrew Doré, Heptares Therapeutics, U.K.

 **Bruker AXS GmbH**  
info.baxs@bruker.com

[www.bruker.com](http://www.bruker.com)

**Worldwide offices**  
[bruker.com/baxs-offices](http://bruker.com/baxs-offices)



**Online information**  
[bruker.com/sc-xrd](http://bruker.com/sc-xrd)

